Published in final edited form as:
J Control Release. 2010 August 17; 146(1): 37–44. doi:10.1016/j.jconrel.2010.05.034.

IN VITRO PERMEATION OF A PEGYLATED NALTREXONE PRODRUG ACROSS MICRONEEDLE-TREATED SKIN

Mikolaj Milewski[a], **Thirupathi Reddy Yerramreddy**[a], **Priyanka Ghosh**[a], **Peter A. Crooks**[a], and **Audra L. Stinchcomb**[a,*]

[a] Department of Pharmaceutical Sciences, College of Pharmacy, University of Kentucky, Lexington, KY 40536-0082, USA

Abstract

Microneedles (MN) are a useful tool for increasing skin permeability to xenobiotics. Previous research showed marked improvement in the percutaneous flux of naltrexone (NTX) hydrochloride by the use of MN skin pretreatment alone; however, for better therapeutic effect, further enhancement is desired. The goal of this *in vitro* study was to combine microneedle skin pretreatment with the use of a highly water-soluble PEGylated naltrexone prodrug (polyethyleneglycol-NTX, PEG-NTX) to investigate its transdermal transport at varying concentrations. Solubility and stability of the prodrug were investigated. *In vitro* diffusion experiments employing MN-treated minipig skin were used to evaluate the performance of the PEGylated prodrug. The results revealed substantial deviation from ideal behavior, with the flux through MN-treated skin having a nonlinear relationship to the prodrug concentration in the donor solution. While in the lower concentration range tested the prodrug flux increase was proportional to the concentration increase, at high concentrations it showed no such dependence. Accounting for the decrease in the effective prodrug diffusivity accompanying the increase in viscosity, as predicted by the Stokes-Einstein equation, provided a rationale for the observed flux values. Increasing the viscosity of the donor solution is hypothesized to afford a curvilinear permeation profile for the PEGylated NTX prodrug.

Keywords

Transdermal drug delivery; microneedles; naltrexone; prodrug; PEGylation

Introduction

The restrictions in percutaneous drug delivery are largely governed by skin anatomy. Skin has evolved to provide an adequate interface between the external and internal body environment, to minimize water loss, and to impede the penetration of xenobiotics. This evolutionary hurdle results in very low skin permeability to most foreign substances [1–3]. The barrier property of the skin for most compounds lies in the stratum corneum (SC) extracellular matrix of lipid bilayers [4,5]. The pool of molecules possessing the necessary physicochemical properties to cross this barrier is limited, and the number of drugs that can

*Corresponding author: Audra L. Stinchcomb, 459 Wethington Bldg., 900 South Limestone Street, Lexington, KY, 40536, Tel: (859) 323 6192, Fax: (859)-257-2787, astin2@email.uky.edu.

be delivered transdermally at therapeutically relevant rates is also low [6]. To overcome this challenge, a variety of different techniques can be used [7,8]. One of the most promising and effective approaches involves the use of microneedles (MN). Micrometer-size needles were shown to be long enough to penetrate the skin effectively breaching the SC barrier, but at the same time being short enough to minimize pain sensation. In general, this process results in up to several orders-of-magnitude enhancement of drug transdermal transport [8,9].

Naltrexone (NTX) is a potent, competitive opioid receptor antagonist used to treat opioid and alcohol addiction [10]. The percutaneous delivery of this agent could bear substantial advantages over currently available dosage forms: i.e. oral tablet and intramuscular controlled-release injection [11,12]. Although neither NTX, nor its active metabolite, 6-β-naltrexol, permeate through skin at clinically relevant rates from reasonably-sized patches [11,12], the use of MN proved to significantly improve transport [13]. Studies have shown that although the creation of microchannels in the skin after MN treatment did not have a substantial effect on the delivery rates of the neutral (free-base) form of NTX or 6-β-naltrexol, an improvement in the delivery of positively charged (salt-form) species of these drugs was possible [13]. It was proposed that higher NTX and 6-β-naltrexol water-solubility at the lower pH range, rather than the presence of a positive charge, was responsible for the observed increase in the transport rates of the salt forms of these drugs [13]. *In vitro* and *in vivo* animal studies proved the utility of the MN method of enhancement showing approximately an order-of-magnitude increase in the transdermal flux of highly water soluble species via MN-assisted delivery over that through untreated skin [13,14]. Subsequently, a first-in-human MN study demonstrated that the combination of MN skin pretreatment and application of four NTX HCl patches afforded drug plasma levels in the lower end of the targeted therapeutic range [15]. Furthermore, an increase in flux would be expected to translate into higher plasma levels, as well as allow a decrease in the number of patches needed.

It is known that PEGylation, or the process of covalent attachment of polyethylene glycol polymer chains to another molecule can substantially increase aqueous solubility of hydrophobic drugs and proteins [16,17]. Besides improved water-solubility, PEGylation is commonly used in the field of pharmaceutics to serve other purposes, such as enhancing stability, modifying pharmacokinetics, shielding labile molecules from proteolytic enzymes, or eliminating protein immunogenicity [18–20]. In the field of transdermal drug delivery, PEGylation has been employed to alter the physicochemical properties of prodrugs to enhance delivery across non-MN-treated skin. Overall, these attempts translated into limited success for passive transdermal delivery. An elevated aqueous solubility was postulated to contribute to a moderate increase in flux observed for some derivatives. All these studies involved drug delivery through non-MN-treated skin [21–23].

Based on the experiments by Banks et al. [13], it could be anticipated that an aqueous solubility increase achieved through PEGylation of NTX would favorably affect flux through MN-enhanced skin. No previous peer-reviewed literature reports have described the transdermal potential of PEGylated drug molecules used in conjunction with MN skin treatment. The aim of this work was to evaluate the *in vitro* transport of a PEGylated NTX prodrug through MN-treated skin, as a function of concentration in the donor solution.

Materials and methods

Chemicals

Naltrexone was purchased from Mallinckrodt (St. Louis, MO, USA). Water was purified using a NANOpure Diamond™ Barnstead water filtration system. Hanks' balanced salts modified powder, and sodium bicarbonate were purchased from Sigma (St. Louis, MO). 4-

(2-Hydroxyethyl)-1-piperazineethanesulfonic acid (HEPES), gentamicin sulfate, trifluoroacetic acid (TFA), triethylamine (TEA), 1-heptane sulfonic acid sodium salt, and acetonitrile (ACN) were obtained from Fisher Scientific (Fairlawn, NJ). 1-Octane sulfonic acid sodium salt was obtained from ChromTech (Apple Valley, MN, USA).

Synthetic procedure for the preparation of the naltrexone PEGylated prodrug (PEG-NTX)

The detailed synthetic procedure for the preparation of 3-O-[3-(2-(2-hydroxyethoxy)ethoxy)propanoyl]naltrexone prodrug has been reported elsewhere [24]. Briefly, to a mixture of naltrexone (0.341 g, 0.001 mol), DMAP (0.146 g, 0.0012 mol), and dicyclohexylcarbodiimide (DCC, 0.247 g, 0.0012 mol) in chloroform (30 ml), 3-(2-(2-hydroxyethoxy)ethoxy)propanoic acid (0.178 g, 0.001 mol) in chloroform (5 ml) solution was added dropwise over a period of 5–10 min under an argon atmosphere at ambient temperature. The solution was stirred at ambient temperature for 24 hrs, then it was cooled to 0–5 °C, and the precipitated dicyclohexyl urea by-product filtered-off. The filtrate was washed with ice-cold water (20 ml), ice-cold brine solution (20 ml), dried over Na_2SO_4, and the solvent evaporated *in vacuo*. The resulting residue was purified by column chromatography (silica gel, eluted with 3% v/v methanol in chloroform) to obtain pure 3-O-[3-(2-(2-hydroxyethoxy)ethoxy)propanoyl]naltrexone (0.42 g, 85% yield) as a colorless oil.

Solubility

The apparent solubilities of the PEG-NTX prodrug and NTX in 0.3M acetate buffer (pH 5.0) were obtained by equilibration of an excess quantity of prodrug/drug in 6ml of buffer. After addition of prodrug/drug, the pH of the resulting slurry was adjusted to pH 5.0, if this was found to be necessary. The PEG-NTX prodrug slurry was continuously shaken in a tightly closed glass vial in a shaking water-bath at 32°C for 12h. A relatively short equilibration time was chosen, due to the hydrolytic instability of the prodrug. The NTX slurry was continuously shaken in a tightly closed glass vial in a shaking water bath at 32°C for 24h. At the end of the equilibration time, samples were transferred to prewarmed plastic centrifuge vials and centrifuged for 10 min at 12000 × g at 32°C. The supernatant was sampled, filtered using a 32°C prewarmed syringe containing a 0.2 μm membrane syringe filter (VWR 28145-491), diluted with an adequate amount of ACN-water 70:30 (v/v), and resulting solution analyzed by high pressure liquid chromatography (HPLC). Solubility determinations were repeated twice (n=2).

Prodrug stability

For the purpose of determining the pH-rate profile, several 20mM buffers were prepared and adjusted to the constant ionic strength of I = 0.1 with NaCl: i.e. pH 2.0 (phosphate buffer), pH 3.3 (citrate buffer), pH 4.4 (formate buffer), pH 5.4 (acetate buffer), pH 5.9 (citrate buffer), pH 6.9 (phosphate buffer) and pH 8.7 (ammonium buffer). A stock solution of PEG-NTX was obtained by dissolving about 40mg of the prodrug in 2 ml ACN. Then, 100μl of the stock solution was transferred to 10ml of buffer thermostated at 32°C, vortexed and filtered through a 0.45μm nylon syringe filter (Acrodisc® Premium 25mm Syringe Filter). Multiple samples were drawn over a period of 140h. Next, prodrug stability studies in donor (0.3M acetate buffer pH 5.0) and receiver solutions (25mM HEPES-buffered Hanks' balanced salt solution pH 7.4) were initiated by charging a 10ml volume of hydrolysis media thermostated at 32°C with ≈1mg of prodrug, filtering the solution through a 0.45μm nylon syringe filter (Acrodisc® Premium 25mm Syringe Filter) and taking samples of the filtrate over a period of 120h. Samples were then diluted with ACN-water 70:30 (v/v) for HPLC analysis. All PEG-NTX-prodrug hydrolysis studies showed pseudo-first-order kinetic behavior. Apparent pseudo-first-order hydrolysis rate constants, k_{app}, were estimated from the slope of the log-transformed amount of PEG-NTX prodrug remaining in the medium. All stability studies were carried out in duplicate (n=2).

Donor solution preparation

Acetate buffer (0.3M, pH 5.0) containing prodrug at saturation (629mM) was diluted with 0.3M acetate buffer, pH 5.0 to obtain solutions at 10, 20, 40, 70 and 90% solubility. Solutions were vortexed and used immediately in *in vitro* diffusion studies.

NTX was added to 0.3M acetate buffer, pH 5.0 to obtain concentrations of 25, 50, 75, 178 and 338mM and the pH of the solutions adjusted to 5.0, if necessary. Solutions were vortexed and used immediately in *in vitro* diffusion studies immediately.

Viscosity measurements

A Brookfield DV-III LV programmable cone/plate rheometer with a CPE-40 spindle was used for measuring the viscosity of the donor solutions. The sample volume was 0.5 ml. All determinations were carried out at 32 °C maintained by a circulating water-bath TC-102. Each donor viscosity measurement was taken three times at low, medium and high torque value in the range of 10–100% of the instrument specifications (n=3).

In vitro diffusion studies

Full-thickness Yucatan minipig skin was harvested from the dorsal region of a euthanized 6-month-old animal. Animal studies were approved by the University of Kentucky IACUC. Subcutaneous fat from skin samples was removed with a scalpel and sparse hair clipped. Such skin samples were immediately placed in a plastic bag and frozen until use (−20°C). The effect of freezing on skin viability [25–27] and permeability to xenobiotics [27–30] has been the subject of multiple studies. The presence [27–29] or absence [30] of freezing-induced increased skin permeability is related to factors such as skin type, nature of the permeant, freezing conditions and time of storage. No major detrimental effect is caused by the freezing of Yucatan minipig skin for up to one year of storage for the purpose of use in *in vitro* drug permeation studies. Before the permeation study, skin samples were allowed to thaw for about 30 min. Skin used for MN treatment was first dermatomed to a thickness of about 1.7mm and then placed on a wafer of polydimethylsiloxane polymer, which mimicked the naturally occurring mechanical support of underlying tissue because of its comparable structural elasticity. In the context of studies described in this article “MN” refers to microneedle rows obtained from Dr. Prausnitz’s laboratory. They were fabricated by laser cutting of stainless steel sheets as reported previously [31]. MN were solid metal, two-dimensional “in-plane” rows each containing five microneedles oriented with their axis parallel to the steel sheet. This design is characterized by the following microneedle dimensions: 750 μm long, 200 μm wide, 75 μm thick and 1.35 mm inter-needle spacing. The insertion of MN into skin was carried out manually by applying gentle finger pressure followed by their instantaneous removal. The diffusion area of skin (0.95 cm^2) was pierced 20 times, with a row containing five microneedles, gradually advancing the MN application area to obtain 100 non-overlapping piercings before mounting the skin in the diffusion cell. If any damage to the MN was observed a new array was used. Three to four cells were used per one drug/prodrug concentration (n=3–4). A PermeGear flow-through (In-Line, Riegelsville, PA) diffusion cell system was used for the *in vitro* diffusion studies. Isotonic HEPES-buffered Hanks’ balanced salts solution (25mM, pH 7.4) was used as the receiver solution. Additional experiments were carried out to ascertain that the receiver flow rate of 1.5 ml/h was sufficient to maintain sink conditions. An increase in flow rate to 7.5ml/h did not change the amount of drug permeating over time, and a lower 1.5ml/h flow rate was used for all experiments for practical convenience. Skin samples in the diffusion cells were maintained at 32°C using a circulating water bath. The diffusion experiments were initiated by charging the donor compartment with 0.4 ml of the donor solution. Samples were collected from the receiver compartment in 6h increments over 48h. All samples were stored at 4°C until HPLC analysis, which was carried out within 24 hours.

Transepidermal water loss (TEWL) measurements

TEWL was used to assess the integrity of the skin barrier using a DermaLab® TEWL probe (CyberDerm Inc.). MN-treatment, by itself, increases TEWL and detection of possible barrier compromise due to vehicle alone under such conditions would be difficult at best. Therefore, a separate diffusion experiment was carried out to evaluate the effect of the drug-free donor solution (0.3M acetate buffer) on the barrier properties of the untreated skin. The TEWL values for uncompromised minipig skin are known, and are generally equal or less than 10 g m^{-2} h^{-1} [32–34]. Measurements were taken after 30 min. equilibration of the untreated skin with the receiver solution in the diffusion apparatus before charging the donor chamber with the drug-free 0.3M pH 5.0 acetate buffer. Another measurement was obtained after removal of the buffer from the donor chamber after 48h, and 30min equilibration.

Prodrug skin disposition

After the completion of the diffusion experiment, skin samples were rinsed three times with distilled water to remove residual formulation and then dismounted from the diffusion cells. A circular section of the skin corresponding to the diffusion area was excised with a scalpel and weighed. Next, the skin sample was placed in a glass vial containing 10ml of ACN, the vial closed tightly and left in a shaking water bath thermostated at 32°C for 12h. Solutions were then sampled, diluted with ACN and analyzed by HPLC. The PEG-NTX prodrug and NTX content was normalized by skin weight and reported as the concentration in the skin.

Quantitative analysis

Quantitative analysis of NTX and the PEG-NTX prodrug by HPLC was carried out using a modification of the assay described by Hussain et al. [35]. The HPLC system consisted of a Waters 717 plus autosampler, a Waters 600 quaternary pump, and a Waters 2487 dual wavelength absorbance detector with Waters Empower™ software. A Waters YMC™ CN column (2.0mm × 150mm) with a CN guard column of the same type (2.0mm × 20mm) was used with the UV detector set at a wavelength of 278nm. The mobile phase consisted of 70:30(v/v) ACN:0.1% TFA containing 0.065% 1-octane sulfonic acid sodium salt, adjusted to pH 3.0 with TEA aqueous phase. Samples were run at a flow rate of 1.5 ml/min with a run time of 4.5 min. The injection volume was 100 μl, and the retention times of PEG-NTX and NTX were 3.2 min and 3.5 min, respectively. Samples were analyzed within a 100–5000ng/ml linear range of the PEG-NTX prodrug and NTX standard curves. Standard solutions exhibited excellent linearity over the entire concentration range employed in the assays.

The permeation data were plotted as the cumulative amount of PEG-NTX and NTX collected in the receiver compartment as a function of time. The steady-state flux value for a given run was calculated from Fick's first law of diffusion from the terminal slope of the cumulative amount plotted against time:

$$\frac{1}{A}\left(\frac{dM}{dt}\right)=J_{ss}=P\times\Delta C \quad (1)$$

where, J_{ss} is the steady-state flux, M is the cumulative amount of drug permeating the skin [nmol], A is the area of the skin [0.95 cm^2], P is the effective permeability coefficient [cm h^{-1}], and ΔC is the concentration difference [nmol cm^{-3}] of the drug in donor and receiver solutions. Since sink conditions prevail under constant flow of the receiver solution, ΔC is well-approximated by the drug donor concentration alone.

Statistical analysis

The statistical analysis of the data was carried out by one-way ANOVA with post-hoc Bonferroni's analysis using SIGMA-STAT software (SPSS, Inc., Chicago, IL, USA).

Results and Discussion

The structures of both parent drug (NTX) and its PEGylated prodrug (PEG-NTX) are presented in Fig. 1.

A short, two ethylene-glycol unit side chain is attached through a hydrolytically labile carboxylate ester linkage to the 3-O position of the NTX molecule. Before the *in vitro* evaluation of the prodrug permeation through the MN-treated skin was carried out, its stability was studied at different pH values. A wide pH range was investigated with the aim of identifying the pH-dependency for slow and fast chemical hydrolysis. The prodrug stability studies at all pH values showed pseudo first-order degradation behavior. Apparent pseudo first-order rate constants (k_{app}) were obtained from the slope of the log-transformed amount of prodrug remaining plotted against time. Fig. 2 summarizes the pH stability in the form of a U-shaped pH-rate profile.

At pH values around 3–5, the PEG-NTX prodrug is most stable. Lower pH values reveal acid-catalyzed hydrolysis while higher pH values demonstrate base-catalyzed hydrolysis. Specifically, in the pH region 7–9, the slope reaches a value of unity, indicating that hydroxide ion-catalyzed hydrolysis is the predominant mechanism of hydrolysis in this pH range. Since under normal conditions, the surface pH of the skin oscillates around 4.5 – 6.0, a donor solution of pH 5.0 was chosen for diffusion experiments to closely mimic the physiological milieu [36,37]. This pH value also provides the best stability for the PEG-NTX prodrug, as indicated by the pH-rate profile. On the other hand, the receiver solution was buffered to the physiologically relevant pH 7.4, reflecting the environment of the deeper layers of skin and bodily fluids [38,39]. Because the actual composition of the donor and receiver solutions differed from buffers used in the stability determination, an additional hydrolysis study was carried out to evaluate PEG-NTX stability in those media. It was found that the prodrug's k_{app} in the donor solution was $1.93 \cdot 10^{-3}$ h^{-1}, which translates into a t_{90} of about 54h, while in the receiver solution k_{app} equaled $2.88 \cdot 10^{-2}$ h^{-1} or a t_{90} of about 4h. In other words, by chemical hydrolysis alone, PEG-NTX would be expected to degrade releasing the parent drug 15 times faster in the receiver solution as compared to the donor solution.. Overall, the t_{90} of over 48h (the duration of diffusion experiment) was deemed to be sufficient to ensure that only a small portion (<10%) of NTX coming from prodrug in the donor solution would be formed, and would not substantially affect the interpretation of the data. Besides stability, the second key parameter of interest was solubility. The main purpose for designing a PEGylated NTX prodrug was to achieve increased water-solubility of the drug in the donor solution. The apparent aqueous solubility values for the parent drug and prodrug were 338mM and 629mM, respectively, showing nearly a 2-fold increase in apparent aqueous solubility of the prodrug compared to that of NTX.

The potential detrimental effect of the acetate buffer (present in donor solution) on skin was evaluated in a separate experiment involving transepidermal water loss (TEWL) measurements before and after charging the donor chamber with the drug-free donor solution over 48h. Typical readings for untreated minipig skin were equal to or less than 10 g m^{-2} h^{-1} [32–34]. The experimental TEWL values for untreated skin remained low and increased from 2.2 ± 0.4 to 3.1 ± 0.2 g m^{-2} h^{-1} over 48h, suggesting no damage to the barrier had occurred. All *in vitro* diffusion experiments used MN-pretreated Yucatan minipig skin. Minipig skin is a well-established model for human skin in transdermal drug delivery as it possesses the characteristics similar to those of the human skin [40,41].

However, as with every model, it has some limitations [42]. Differences in the structure of the dermis may translate into a different diffusional resistance of that tissue, and therefore affect the flux values obtained from MN-enhanced permeation experiments. The diagram of the experimental set-up used to investigate the transport of PEG-NTX prodrug across MN-treated skin is presented in Fig. 3.

The transdermal permeation through MN-enhanced skin was evaluated at 6 concentrations for PEG-NTX: i.e. 10, 20, 40, 70, 90 and 100% saturation, or 63, 126, 252, 440, 566 and 629mM. The saturated solution did not contain any undissolved prodrug to ensure that potential interference between excess prodrug and microchannels, such as obstruction of the microchannel opening, presence of the undissolved prodrug in the microchannels, etc., would not affect the results. Since the prodrug possesses much lower chemical stability at elevated pHs, its diffusion across MN-treated skin is accompanied by simultaneous chemical hydrolysis and possibly enzymatic bioconversion. As a result, two species, the prodrug itself and NTX generated from hydrolysis of the prodrug, are detectable in the receiver solution. Prodrug permeation from donor solution at either concentration tested resulted in steady-state conditions after a relatively short lag time. A representative permeation profile is presented in Fig. 4 and permeation data is summarized in Table 1.

The total flux was obtained by summation of prodrug flux and NTX-from-prodrug flux, and can be seen as a measure of overall performance of the prodrug. Steady-state total flux values plotted as a function of PEG-NTX concentration in the donor are shown in Fig. 5. (Note that Table 1 reports flux of unhydrolyzed (intact) PEG-NTX prodrug and NTX-from prodrug separately while Fig. 5 sums them up to obtain total PEG-NTX prodrug flux (filled circles) which is contrasted with the flux of NTX alone obtained from a separate experiment).

While in the lower concentration range (63–252mM) the increase in the flux is roughly proportional to the increase in concentration, at higher concentrations (440–629mM) the flux is independent, if not inversely related, to the donor concentration. The behavior in the low concentration range can be well predicted by using Fick's first law of diffusion and a concentration-independent permeability coefficient. However, the deviation from ideal behavior is substantial in the higher concentration range. Additionally, Fig. 5 illustrates the permeation of the parent drug alone from data obtained from a separate experiment. NTX alone provides higher flux as compared to the PEG-NTX prodrug at any corresponding concentration. The permeability coefficient of the prodrug is expected to be somewhat lower than the permeability coefficient of the parent drug, due to its higher molecular weight. In bulk solution (as in microchannels), the Stokes-Einstein equation can be used to inversely relate solute diffusivity to the cubic root of the size of a molecule, $D \sim MW^{-0.33}$. On the other hand, in dermis, Kretos et al. found that the Wilke-Chang relationship, which predicts a steeper drop in diffusivity as a function of increasing molecular weight, $D \sim MW^{-0.6}$, correlated well with their experimental data [43]. However, other functional relationships including that predicted by the Stokes-Einstein equation were not excluded. In other words an increase in the molecular weight from 341 Da (parent drug) to 502 Da (PEG-NTX prodrug) would be expected to decrease prodrug diffusivity by about 12% (by the Stokes-Einstein equation) or about 20% (by the Wilke-Chang relationship). Furthermore, the hydrodynamic radius of the PEG-NTX prodrug may be actually larger than that calculated from the molecular weight alone due to the association of water molecules with the PEG chain. Overall, superior prodrug solubility, even with a somewhat decreased diffusivity, but in the absence of non-ideal behavior, should result in improved transdermal flux through MN-treated skin.

It has been suggested that the viscosity of the donor solution may have a vital effect on drug delivery rates through MN-treated skin [44]. The relationship between the viscosity (η) of the diffusion medium and the diffusion coefficient is given by the Stokes-Einstein equation:

$$D=\frac{kT}{6\pi\eta r} \tag{2}$$

where k is Boltzmann's constant, T is absolute temperature, and r is the radius of the diffusant (assuming it can be represented by a spherical particle). Specifically, it was shown that the NTX HCl flux through microchannels and underlying dermis correlated well with the decrease in the calculated drug diffusivity in the donor solution. Additionally, the flux through microchannels using aqueous drug solutions was found to be well approximated by the flux through MN-enhanced skin (the contribution of flux through skin around microchannels was low). To test the hypothesis that an increase in the viscosity of the prodrug-containing donor solution may explain low PEG-NTX flux at high concentrations, the donor solution viscosity values were measured. It is known that at sufficiently high solute concentration, solvent viscosity can be altered, exerting a secondary effect on the solute's own diffusivity [45]. Fig. 6 shows that donor solution viscosity increases in an exponential fashion as a function of the prodrug concentration, and demonstrates approximately a 3-fold increase between the lowest and highest concentrations tested.

A simple log-linear empirical equation in the form of:

$$\log\eta=a\times C+b \tag{3}$$

was used to describe this trend for later flux calculations, where C is concentration [mM] and a and b are fitted parameters [46]. The experimental data can be transformed by normalizing either flux or permeability coefficient for apparent viscosity effect. Multiplication by viscosity of a given donor solution affords the viscosity normalized parameter, e.g.

$$J'=J\times\eta \tag{4}$$

or

$$P'=P\times\eta \tag{5}$$

where J′ is the viscosity-normalized flux, J is the experimentally measured flux and is the viscosity of the donor solution, and the P′ is the viscosity-normalized permeability coefficient and P is the experimentally determined permeability coefficient. Such correction results in flux or permeability coefficient values corresponding to a viscosity value of unity. If the hypothesis is valid, it would be expected that the viscosity-normalized flux will correlate linearly with the prodrug concentration in the donor solution over the whole concentration range tested. A plot of viscosity-normalized flux is presented in Fig. 7, which shows a reasonable linear correlation ($R^2 = 0.96$).

Moreover, from the slope of this graph, an average viscosity-normalized permeability coefficient P'_{ave} of $23.01 \cdot 10^{-5} \pm 2.57 \cdot 10^{-5}$ (mean ± 95% CI) was estimated. Individual viscosity-normalized permeability coefficients (P′) are reported in Table 2.

Apart from the P′ for the 63mM concentration which is somewhat higher than the average, the normalized permeability coefficients are concentration-independent over the range of prodrug concentrations tested (one way ANOVA with post-hoc Bonferroni's analysis reveals a statistically significant difference at $\alpha = 0.05$ between the P′ at 63mM and P′ at 629mM). In other words, the changes in MN-enhanced percutaneous flux of the PEG-NTX prodrug can be satisfactorily explained by changes in the viscosity of the donor solution.

Assuming that most prodrug molecules permeate through microchannels and into the dermis below, rather than through skin around microchannels, a two-ply membrane concept incorporating the microchannel and underlying dermis can be used to rationalize the data. In the experimental set-up used in the current study the thickness of the dermis below the microchannel exceeds the length of the microchannel, and the diffusion coefficients of drugs in the dermis are known to be approximately 3.7-fold lower as compared to those in the bulk aqueous solutions [43]. Based on the above, it can be expected that the major diffusional resistance lies in the dermis layer. Therefore, flux should not depend on the viscosity of the donor solution unless it changes the properties of the barrier (dermis). It is possible that the prodrug-containing, elevated-viscosity donor solution alters the microenvironment of the dermis by increasing its diffusional resistance. Assuming this effect is similar to that seen in the bulk solution, flux through microchannels and dermis below would be inversely related to the viscosity of the donor solution. In other words, the results from the current study imply that changes in the prodrug diffusivity in the donor solution are reflective of prodrug diffusivity changes in the whole skin barrier. Using the previously estimated average viscosity-normalized permeability coefficient (P'_{ave}) and the viscosity of the donor solution at any given concentration, an expected flux (J_{calc}) can be calculated from:

$$J_{calc} = \frac{P'_{ave}}{\eta} \times C \tag{6}$$

which, after incorporation of equation (3), becomes:

$$J_{calc} = \frac{P'_{ave}}{10^{(0.000807 \times C - 0.097641)}} \times C \tag{7}$$

where C is the prodrug donor concentration [mM]. Fig. 8 presents experimental data and compares it to the predicted total flux for the PEG-NTX prodrug. A reasonable agreement between experimental and calculated values lends practical utility to this approach.

Finally, prodrug skin disposition studies at the end of the diffusion experiment were carried out. Both prodrug and NTX-from-prodrug were detected in the skin. Table 3 shows the amount of each as a function of changing concentrations in the donor solution.

The extent of prodrug metabolism, calculated as fraction of prodrug converted to NTX, does not differ substantially and remains constant at 37 ± 10%. This value is somewhat higher that its counterpart (29 ± 9%) obtained from flux values (Table 1), and likely reflects extra degradation that occurred during sample processing time and skin extraction procedures. A lack of decline in the fraction of prodrug metabolized with an increase in concentration suggests either chemical hydrolysis alone or chemical hydrolysis accompanied by non-saturable enzymatic hydrolysis is the primary mechanism for PEG-NTX hydrolysis in skin.

Conclusions

The current study explored the *in vitro* permeation of a PEGylated NTX prodrug across MN-treated skin as a function of its concentration in the donor solution. It has been found that the flux did not proportionally increase when high concentrations of the prodrug in the donor solution were utilized. In other words, the apparent permeability coefficient (calculated as a ratio of flux over drug concentration in the donor solution) is not a concentration-independent proportionality constant between flux and drug concentration. It was hypothesized that this non-linearity was caused by elevated viscosity of the donor media. Calculations based on the Stokes-Einstein equation afford a reasonable explanation of the experimental data. Interestingly, if this reasoning is correct, a clear decline in flux would be expected with further increases in prodrug concentrations in the donor solution. It was not possible to investigate this with the present PEG-NTX prodrug, due to its limited solubility. Overall, it cannot be excluded that other formulation characteristics besides viscosity of the donor solution may also alter transport rates through MN-treated skin. Apart from kinetics considerations, a decrease in the thermodynamic chemical potential of the diffusant at high concentrations may also contribute to deviation from ideal behavior. Nevertheless, in the present study, accounting for changes in viscosity alone provided a rational interpretation for the data obtained. Obviously, the generalization of the results obtained from the current study will require further investigation. It is not expected that the type of behavior seen in the present study will be universal for all MN-involving transport experiments as different methods of MN application, MN design and formulation characteristics play a significant role in the drug transport across MN-treated skin [47]. In consequence, the generality of the present *in vitro* findings may be limited to the studies involving water-based formulations, MN-pretreated skin with microchannels having similar characteristics to those obtained in this study, and permeants which cross the skin mainly through microchannels and underlying dermis, rather than through the intact skin around microchannels.

Acknowledgments

The authors would like to thank Dr. Mark Prausnitz and Dr. Vladimir Zarnitsyn of Georgia Tech for providing the MN and expert advice. This research was supported by NIDA R01 DA13425.

References

1. Elias, FKPM.; Fluhr, JW. Mc-Graw Hill. Freedberg, EAIM.; Wolff, K.; Austen, KF.; Goldsmith, LA.; Katz, SI., editors. New York: 2003.
2. Madison KC. Barrier function of the skin: “La raison d’etre” of the epidermis. J Invest Dermatol. 2003; 121(2):231–241. [PubMed: 12880413]
3. Harding Clive R. The stratum corneum: structure and function in health and disease. Dermatologic therapy. 2004; 17(Suppl 1):6–15. [PubMed: 14728694]
4. Michaels AS, Chandrasekaran SK, Shaw JE. Drug permeation through human skin. Theory and in vitro experimental measurement. AIChE Journal. 1975; 21(5):985–996.
5. Tojo K. Random brick model for drug transport across stratum corneum. J Pharm Sci. 1987; 76(12): 889–891. [PubMed: 3440932]
6. Prausnitz MR, Mitragotri S, Langer R. Current status and future potential of transdermal drug delivery. Nature Reviews Drug Discovery. 2004; 3(2):115–124.
7. Arora A, Prausnitz MR, Mitragotri S. Micro-scale devices for transdermal drug delivery. Int J Pharm. 2008; 364(2):227–236. [PubMed: 18805472]
8. Prausnitz MR, Langer R. Transdermal drug delivery. Nature Biotechnology. 2008; 26(11):1261–1268.

9. Henry S, McAllister DV, Allen MG, Prausnitz MR. Microfabricated Microneedles: A Novel Approach to Transdermal Drug Delivery. Journal of Pharmaceutical Sciences. 1998; 87(8):922–925. [PubMed: 9687334]
10. Volpicelli JR, Rhines KC, Rhines JS, Volpicelli LA, Alterman AI, O'Brien CP. Naltrexone and alcohol dependence. Role of subject compliance. Arch Gen Psychiatry. 1997; 54(8):737–742. [PubMed: 9283509]
11. Paudel KS, Nalluri BN, Hammell DC, Valiveti S, Kiptoo P, Hamad MO, Crooks PA, Stinchcomb AL. Transdermal delivery of naltrexone and its active metabolite 6-beta-naltrexol in human skin in vitro and guinea pigs in vivo. Journal of Pharmaceutical Sciences. 2005; 94(9):1965–1975. [PubMed: 16052561]
12. Valiveti S, Paudel KS, Hammell DC, Hamad MO, Chen J, Crooks PA, Stinchcomb AL. In Vitro/in Vivo Correlation of Transdermal Naltrexone Prodrugs in Hairless Guinea Pigs. Pharmaceutical Research. 2005; 22(6):981–989. [PubMed: 15948042]
13. Banks SL, Pinninti RR, Gill HS, Crooks PA, Prausnitz MR, Stinchcomb AL. Flux Across Microneedle-treated Skin is Increased by Increasing Charge of Naltrexone and Naltrexol In Vitro. Pharmaceutical Research. 2008; 25(7):1677–1685. [PubMed: 18449628]
14. Banks SL, Paudel KS, Pinninti RR, Gill HS, Crooks PA, Brogden NK, Prausnitz MR, Stinchcomb AL. Transdermal Delivery of Naltrexol and Skin Permeability Lifetime after Microneedle Treatment in Hairless Guinea Pigs In Vivo. Journal of Pharmaceutical Sciences. 2010 In press.
15. Wermeling DP, Banks SL, Hudson DA, Gill HS, Gupta J, Prausnitz MR, Stichcomb AL. Microneedles permit transdermal delivery of a skin-impermeant medication to humans. Proceedings of the National Academy of Sciences of the United States of America. 2008; 105(6): 2058–2063. [PubMed: 18250310]
16. Bruckdorfer T. PEGylation - a key technology to improve solubility and pharmacokinetic of peptides, proteins and other biopharmaceuticals for superior drug delivery. Biopolymers. 2009; 92(4):337–337.
17. Riley T, Riggs-Sauthier J. The benefits and challenges of PEGylating small molecules. Pharmaceutical Technology. 2008; 32(7):88, 90–92, 94.
18. Basu A, Yang K, Wang ML, Liu S, Chintala R, Palm T, Zhao H, Peng P, Wu DC, Zhang ZF, Hua J, Hsieh MC, Zhou J, Petti G, Li XG, Janjua A, Mendez M, Liu J, Longley C, Zhang Z, Mehlig M, Borowski V, Viswanathan M, Filpula D. Structure-function engineering of interferon-beta-1b for improving stability, solubility, potency, immunogenicity, and pharmacokinetic properties by site-selective mono-PEGylation. Bioconjugate Chemistry. 2006; 17(3):618–630. [PubMed: 16704199]
19. Harris JM, Chess RB. Effect of PEGylation on pharmaceuticals. Nature Reviews Drug Discovery. 2003; 2(3):214–221.
20. Veronese FM, Pasut G. PEGylation, successful approach to drug delivery. Drug Discovery Today. 2005; 10(21):1451–1458. [PubMed: 16243265]
21. Bonina FP, Puglia C, Barbuzzi T, de Caprariis P, Palagiano F, Rimoli MG, Saija A. In vitro and in vivo evaluation of polyoxyethylene esters as dermal prodrugs of ketoprofen, naproxen and diclofenac. European Journal of Pharmaceutical Sciences. 2001; 14(2):123–134. [PubMed: 11500258]
22. Thomas JD, Majumdar S, Sloan KB. Soft alkyl ether prodrugs of a model phenolic drug: the effect of incorporation of ethyleneoxy groups on transdermal delivery. Molecules. 2009; 14(10):4231–4245. [PubMed: 19924060]
23. N'Da DD, Breytenbach JC. Synthesis of methoxypoly(ethylene glycol) carbonate prodrugs of zidovudine and penetration through human skin in vitro. Journal of Pharmacy and Pharmacology. 2009; 61(6):721–731. [PubMed: 19505362]
24. Yerramreddy TR, Milewski M, Penthala NR, Stinchcomb AL, Crooks PA. Design and Synthesis of Novel 3-O-Pegylated Carboxylate and 3-O-Pegylated Carbamate Prodrugs of Naltrexone for Microneedle-Enhanced Transdermal Delivery Molecules. 2010 In Press.
25. Wester RC, Christoffel J, Hartway T, Poblete N, Maibach HI, Forsell J. Human cadaver skin viability for in vitro percutaneous absorption: Storage and detrimental effects of heat-separation and freezing. Pharmaceutical Research. 1998; 15(1):82–84. [PubMed: 9487551]

26. Messager S, Hann AC, Goddard PA, Dettmar PW, Maillard JY. Assessment of skin viability: is it necessary to use different methodologies? Skin Res Technol. 2003; 9(4):321–330. [PubMed: 14641882]
27. Shaikh NA, Ademola JI, Maibach HI. Effects of freezing and azide treatment of in vitro human skin on the flux and metabolism of 8-methoxypsoralen. Skin Pharmacol. 1996; 9(4):274–280. [PubMed: 8896119]
28. Ahlstrom LA, Cross SE, Mills PC. The effects of freezing skin on transdermal drug penetration kinetics. J Vet Pharmacol Ther. 2007; 30(5):456–463. [PubMed: 17803739]
29. Babu RJ, Kanikkannan N, Kikwai L, Ortega C, Andega S, Ball K, Yim S, Singh M. The influence of various methods of cold storage of skin on the permeation of melatonin and nimesulide. Journal of Controlled Release. 2003; 86(1):49–57. [PubMed: 12490372]
30. Moody RP, Yip A, Chu I. Effect of Cold Storage on In Vitro Human Skin Absorption of Six 14C-Radiolabeled Environmental Contaminants: Benzo[a]Pyrene, Ethylene Glycol, Methyl Parathion, Naphthalene, Nonyl Phenol, and Toluene. J Toxicol Env Health Part A. 2009; 72(8):505–517. [PubMed: 19267311]
31. Gill HS, Prausnitz MR. Coated microneedles for transdermal delivery. J Controlled Release. 2007; 117(2):227–237.
32. Chilcott RP, Stubbs B, Ashley Z. Habituating pigs for in-pen, non-invasive biophysical skin analysis. Laboratory animals. 2001; 35(3):230–235. [PubMed: 11459406]
33. Gendimenico GJ, Liebel FT, Fernandez JA, Mezick JA. Evaluation of topical retinoids for cutaneous pharmacological activity in Yucatan microswine. Archives of Dermatological Research. 1995; 287(7):675–679. [PubMed: 8534132]
34. Kanikkannan N, Burton S, Patel R, Jackson T, Sudhan Shaik M, Singh M. Percutaneous permeation and skin irritation of JP-8+100 jet fuel in a porcine model. Toxicology Letters. 2001; 119(2):133–142. [PubMed: 11311575]
35. Hussain MA, Koval CA, Myers MJ, Shami EG, Shefter E. Improvement of the oral bioavailability of naltrexone in dogs: a prodrug approach. J Pharm Sci. 1987; 76(5):356–358. [PubMed: 3656096]
36. Yosipovitch G, Xiong GL, Haus E, Sackett-Lundeen L, Ashkenazi I, Maibach HI. Time-dependent variations of the skin barrier function in humans: transepidermal water loss, stratum corneum hydration, skin surface pH, and skin temperature. J Invest Dermatol. 1998; 110(1):20–23. [PubMed: 9424081]
37. Firooz A, Gorouhi F, Davari P, Atarod M, Hekmat S, Rashighi-Firoozabadi M, Solhpour A. Comparison of hydration, sebum and pH values in clinically normal skin of patients with atopic dermatitis and healthy controls. Clinical and experimental dermatology. 2007; 32(3):321–322. [PubMed: 17335552]
38. Buraczewska, I. Dry Skin and Moisturizers. 2. 2006. Outside and inside skin pH; p. 161-169.
39. Ohman H, Vahlquist A. The pH gradient over the stratum corneum differs in X-linked recessive and autosomal dominant ichthyosis: a clue to the molecular origin of the “acid skin mantle”? J Invest Dermatol. 1998; 111(4):674–677. [PubMed: 9764852]
40. Fujii M, Yamanouchi S, Hori N, Iwanaga N, Kawaguchi N, Matsumoto M. Evaluation of yucatan micropig skin for use as an in vitro model for skin permeation study. Biological & Pharmaceutical Bulletin. 1997; 20(3):249–254. [PubMed: 9084881]
41. Eggleston TA, Roach WP, Mitchell MA, Smith K, Oler D, Johnson TE. Comparison of two porcine (Sus scrofa domestica) skin models for in vivo near-infrared laser exposure. Comparative Medicine. 2000; 50(4):391–397. [PubMed: 11020157]
42. Gore AV, Liang AC, Chien YW. Comparative biomembrane permeation of tacrine using Yucatan minipigs and domestic pigs as the animal model. Journal of Pharmaceutical Sciences. 1998; 87(4): 441–447. [PubMed: 9548896]
43. Kretsos K, Miller MA, Zamora-Estrada G, Kasting GB. Partitioning, diffusivity and clearance of skin permeants in mammalian dermis. Int J Pharm. 2008; 346(1–2):64–79. [PubMed: 17703903]
44. Milewski M, Stinchcomb AL. Vehicle composition influence on the microneedle-enhanced transdermal flux of naltrexone hydrochloride. Pharm Res. 2010 In press.
45. Flynn GL, Yalkowsky SH, Roseman TJ. Mass transport phenomena and models. Theoretical concepts. Journal of Pharmaceutical Sciences. 1974; 63(4):479–510. [PubMed: 4828694]

46. Chirife J, Buera MP. A Simple Model for Predicting the Viscosity of Sugar and Oligosaccharide Solutions. Journal of Food Engineering. 1997; (33):221–226.

47. Milewski M, Brogden NK, Stinchcomb AL. Current aspects of formulation efforts and pore lifetime related to microneedle treatment of skin. Expert Opinion on Drug Delivery. 7(5):617–629. [PubMed: 20205604]

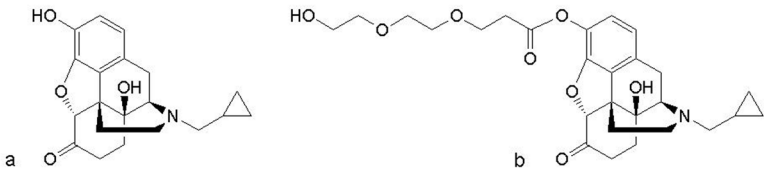

Fig. 1.
Structures of (a) naltrexone and (b) its PEGylated prodrug.

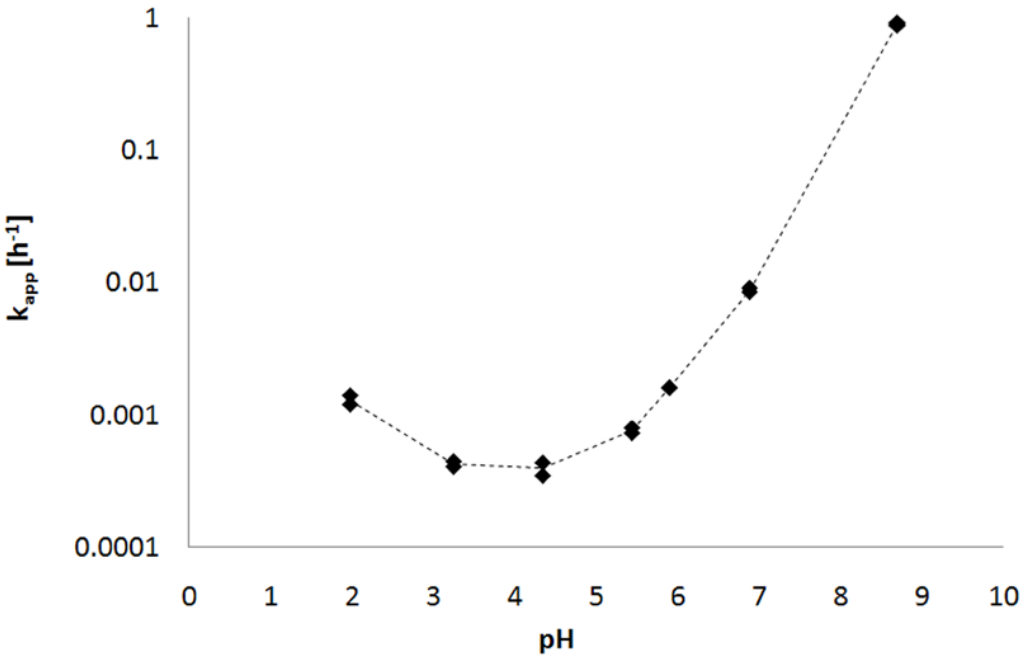

Fig. 2.

pH-rate profile for the hydrolysis of the PEG-NTX prodrug ester bond in 20mM buffers, I=0.1 at 32°C. Points indicate apparent rate constants for the degradation of the prodrug (n=2).

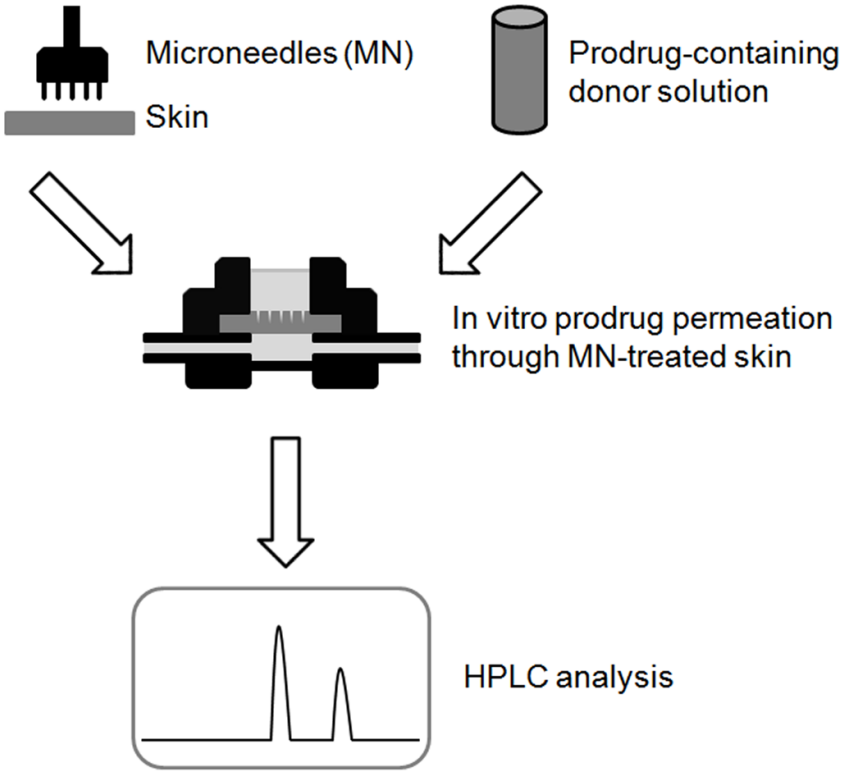

Fig 3.

Diagram of the *in vitro* experimental set-up used to study the permeation of the PEG-NTX prodrug. Yucatan minipig skin was treated with MN to obtain 100 microchannels and mounted into a diffusion cell. Six different concentrations of the prodrug solution (pH 5.0) were prepared and placed in diffusion cell donor compartments to initiate the permeation experiment. Fractions of the receiver solution composed of the isotonic HEPES-buffered Hanks' balanced salts solution (pH 7.4) were collected every 6h over the 48h duration of the experiment. They were analyzed by HPLC for the presence of the PEG-NTX prodrug (intact prodrug) and the NTX-from-prodrug (parent drug generated from prodrug).

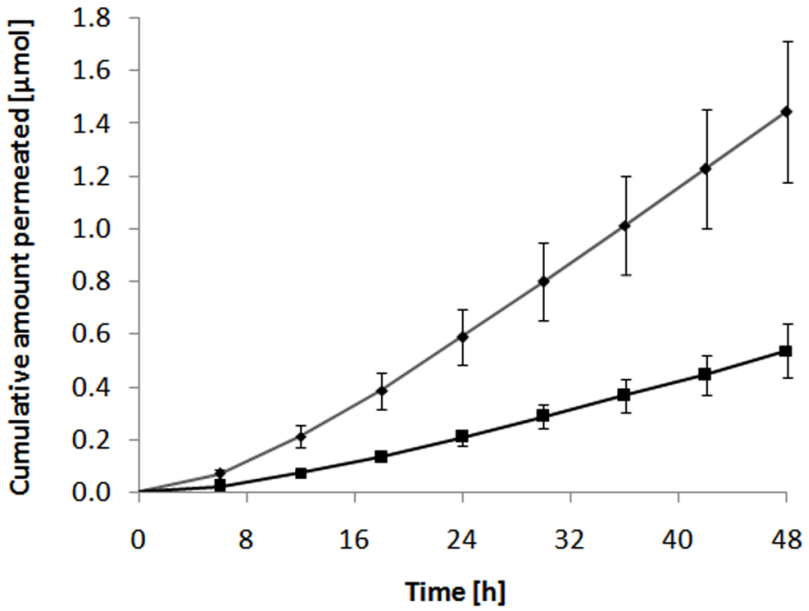

Fig. 4.

Representative *in vitro* permeation profile of the PEG-NTX prodrug through MN-treated Yucatan minipig skin. The cumulative amount of PEG-NTX prodrug itself (◆) and NTX generated from the prodrug (■) detected in the receiver phase are plotted against time. Each point represents the mean ± SD (n=4).

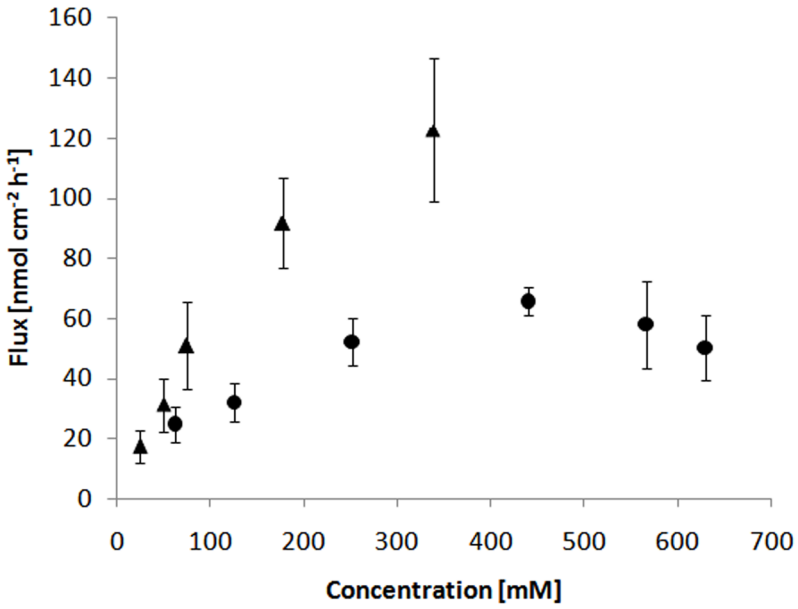

Fig. 5.

Summary of the drug permeation data presented as a total flux plotted against drug concentration in the donor solution. Two independent plots correspond to two separate experiments which used either: PEG-NTX prodrug (●) or NTX (▲) as the permeant in the donor solution. MN-treated Yucatan minipig skin was employed. Each point represents the mean ± SD (n=3–4).

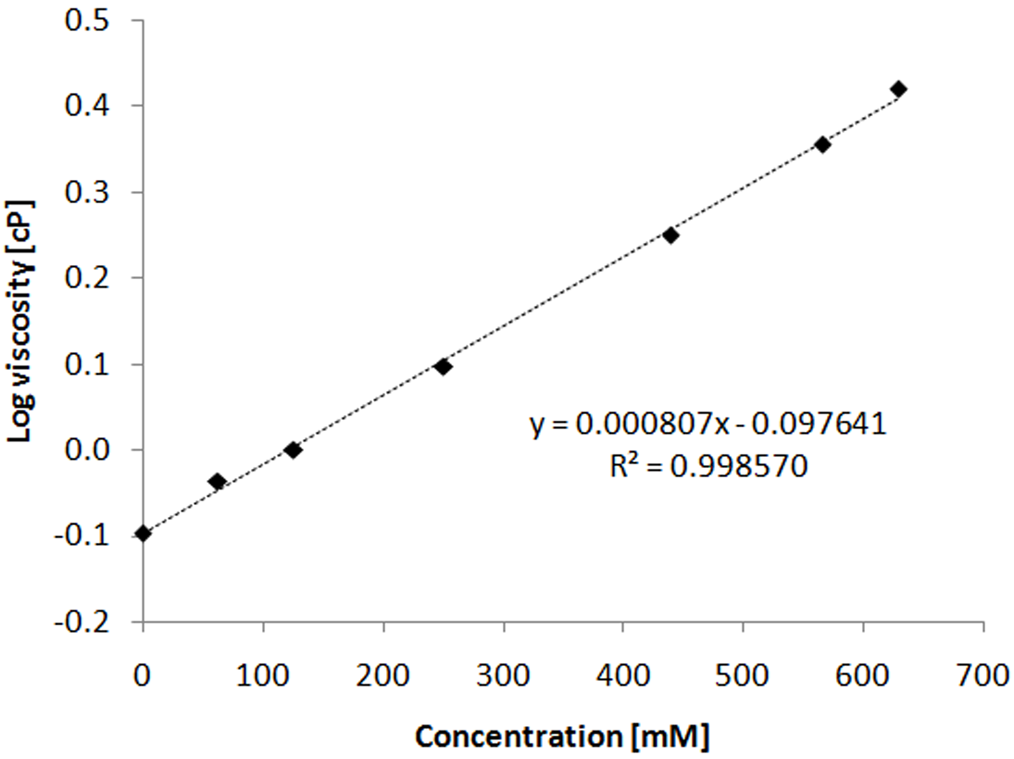

Fig. 6.

Viscosity of the prodrug-containing donor solutions as a function of PEG-NTX prodrug concentration. Points indicate experimentally measured viscosity values while dashed line represents the least-squares fit to the log-linear empirical equation (3). Each point represents the mean of three determinations (n=3), standard deviation is smaller than the size of the symbols.

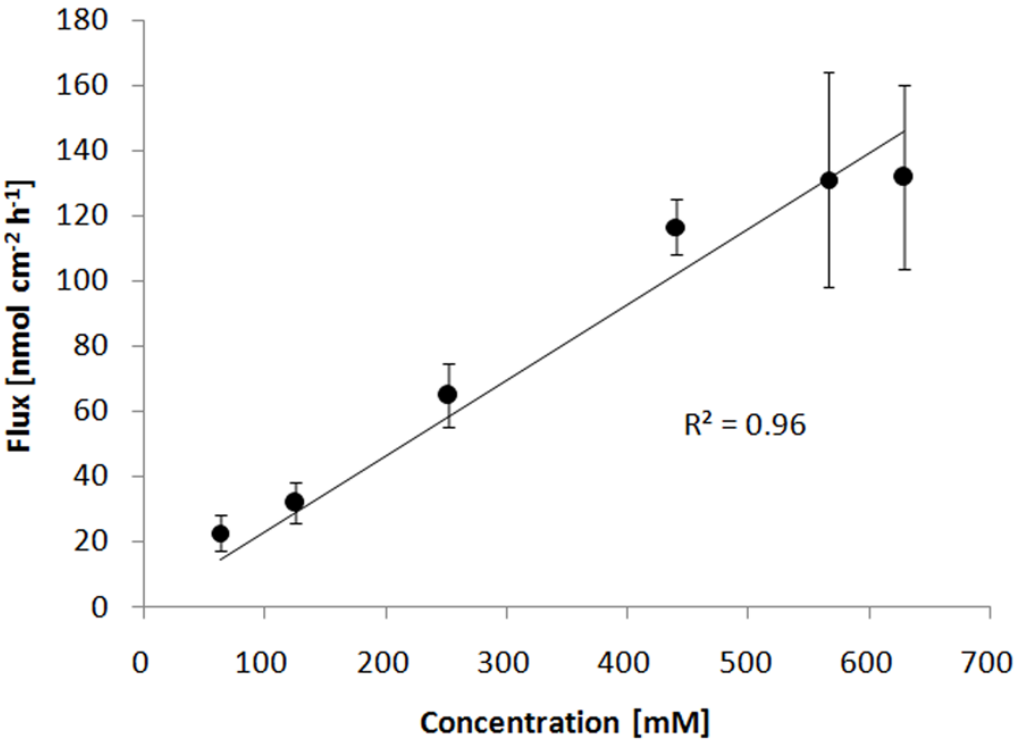

Fig. 7.

Total flux of the PEG-NTX prodrug through MN-treated Yucatan minipig skin normalized per viscosity of the donor solution according to equation (4). Points indicate calculated viscosity-normalized total flux values and solid line represents the least-square fit to a linear equation with zero Y-intercept. Each point represents the mean ± SD (n=3–4).

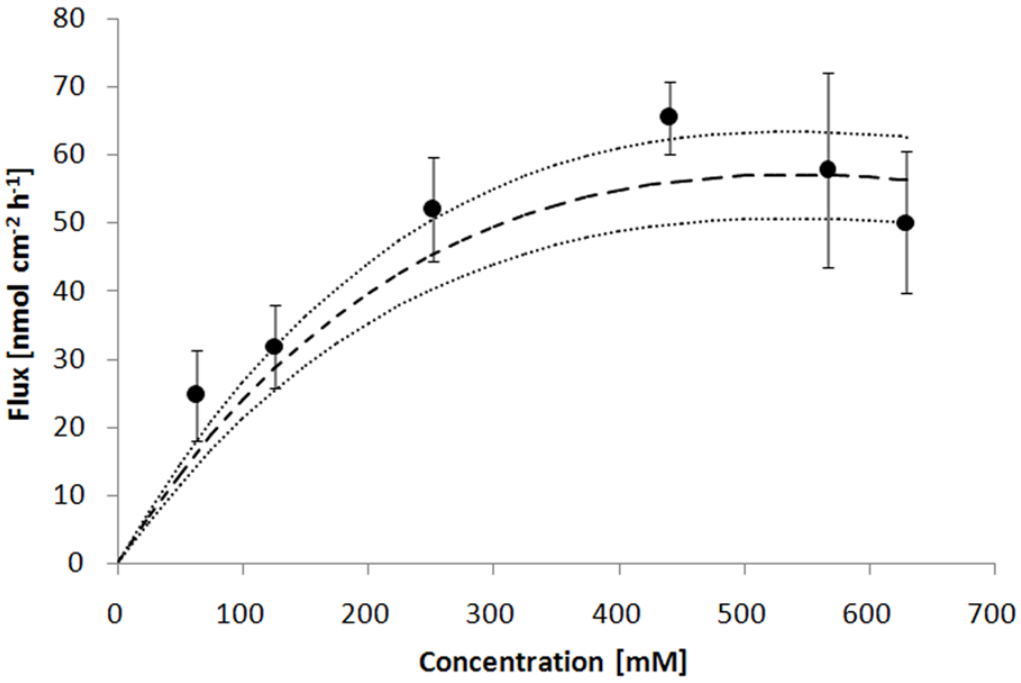

Fig. 8.

Comparison of the experimental total prodrug flux through MN-treated Yucatan minipig skin to the flux calculated according to the equation (7). Points indicate experimentally measured mean flux values ± 95% CI (n=3–4) and dashed line denotes the calculated mean flux value ± 95% CI as outlined by dotted lines.

Table 1

Summary of the *in vitro* permeation of the PEG-NTX prodrug through MN-treated Yucatan minipig skin from donor solutions containing prodrug at different concentrations. Simultaneous diffusion and hydrolysis of the prodrug resulted in the detection of both: prodrug itself and NTX-from-prodrug in the receiver phase. Each value represents the mean ± SD (n=3–4).

Prodrug concentration in donor solution [mM]	Prodrug		NTX-from-prodrug		Fraction of prodrug converted ± SD [%]	n
	Flux ± SD [nmol cm^{-2} h^{-1}]	Lag time ± SD [h]	Flux ± SD [nmol cm^{-2} h^{-1}]	Lag time ± SD [h]		
63	17.9 ± 5.3	5.8 ± 0.7	6.8 ± 2.5	10.5 ± 1.1	28 ± 12	3
126	22.9 ± 5.7	8.4 ± 2.6	9.0 ± 2.5	9.5 ± 2.2	28 ± 10	4
252	37.9 ± 7.3	7.8 ± 1.0	14.1 ± 2.8	8.6 ± 1.1	27 ± 7	4
440	45.0 ± 4.1	7.7 ± 0.6	20.5 ± 2.3	12.0 ± 1.7	31 ± 4	3
566	40.8 ± 13.8	4.2 ± 2.3	17.0 ± 4.8	8.6 ± 1.5	29 ± 11	4
629	35.5 ± 10.1	3.5 ± 2.7	14.6 ± 3.6	7.8 ± 2.9	29 ± 9	4

Table 2

Summary of individual permeability coefficients (P) and viscosity-normalized permeability coefficients (P′) as a function of the prodrug concentration in the donor solution. Permeability coefficients were normalized per viscosity according to equation (5). Each value represents the mean ± SD (n=3–4).

Prodrug donor concentration [mM]	**63**	**126**	**252**	**440**	**566**	**629**
n	3	4	4	3	4	4
$P \times 10^5 \pm SD$ [cm h^{-1}]	39.3 ± 9.3	25.4 ± 4.9	20.7 ± 3.1	14.9 ± 1.1	10.2 ± 2.6	8.0 ± 1.7
$P' \times 10^5 \pm SD$ [cm h^{-1}]	36.1 ± 8.6	25.4 ± 4.9	25.9 ± 3.9	26.5 ± 1.9	23.2 ± 5.9	21.0 ± 4.5

Table 3

Summary of the drug skin disposition at the end of the 48h diffusion experiment involving MN-treated Yucatan minipig skin. Both the PEG-NTX prodrug and NTX-from-prodrug were detected in the skin. Each value represents the mean ± SD (n=3–4).

Prodrug donor concentration [mM]	**63**	**126**	**252**	**440**	**566**	**629**
n	3	4	4	3	4	4
Prodrug amount ± SD [nmol/g skin]	367 ± 127	597 ± 214	850 ± 306	1445 ± 123	1352 ± 125	1459 ± 236
NTX from prodrug amount ± SD [nmol/g skin]	253 ± 54	404 ± 129	504 ± 189	752 ± 68	749 ± 68	784 ± 87